RSC Advances

ROYAL SOCIETY OF CHEMISTRY

www.rsc.org/advances

Table of Contents Graphic

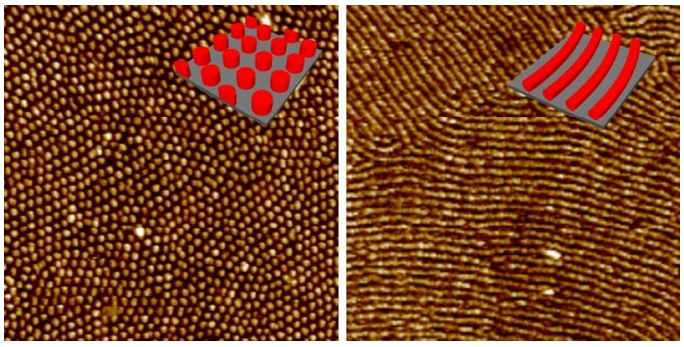

Topographic nanopatterns of fluorescent cylinders in hexagonal order and in parallel line are demonstrated with the utilization of fluorophore-functionalized diblock copolymers.

Fluorescent Topographic Nanopatterns by Fluorophore-Functionalized Diblock Copolymers

Jin-Kyung Lee, Heejung Kang, Sanghwa Lee, Inho Choi, and Byeong-Hyeok Sohn*

Department of Chemistry, Seoul National University, Seoul 151-747, Korea

E-mail: bhsohn@snu.ac.kr

Keywords: Fluorescence, Topographic Nanopattern, Diblock Copolymer

Abstract

We demonstrated the fabrication of fluorophore-functionalized nanopatterns with topographic features. To obtain fluorescent nanopatterns, diblock copolymers having fluorophores in one of the blocks were synthesized by the reversible addition fragmentation chain transfer polymerization and were annealed by solvent vapor, resulting in perpendicular or parallel cylindrical nanopatterns functionalized with fluorophores, depending on the annealing solvent. Then, by etching one of the blocks of copolymers, we were able to produce fluorescent topographic nanopatterns. Furthermore, Au nanorods selectively loaded in the nanometer-sized valley of the pattern effectively altered the fluorescence of the topographic nanopattern.

1. Introduction

Nanometer-sized fluorophores such as dye-functionalized nanoparticles and quantum dots have been largely investigated for various applications including chemical or biological detection,[1,2] imaging,[3,4] and labeling.[5,6] For example, organic fluorescent molecules were isolated and stabilized by silica nanoparticles, which were efficiently utilized for bio-imaging and cell labeling.[7] Most of the applications with nano-scale fluorophores have been performed in solutions. However, their applications can be extended to solid-state devices such as chemical and biological sensors if they are arranged or patterned on solid substrates. For instance, quantum dots were fixed on a solid substrate for effective cell detection.[8,9] Particularly nano-scale patterning of fluorophores is desirable to achieve high sensitivity. Many patterning methods including printing[10,11] and electrostatic deposition[12] can allow direct fabrication of patterns of quantum dots and fluorophore-functionalized nanoparticles but mostly in the micrometer scale. Top-down lithographic techniques combined with fluorophore-functionalized photoresists can be employed to create fluorescent patterns,[13-15] which have also a limit for production of nanometer-sized patterns.

As an alternative or a complimentary method to top-down lithographic techniques for nanoscale patterns, utilization of self-assembled nanostructures of block copolymers has been considered. Block copolymers, consisting of two or more polymers covalently connected, spontaneously assemble into various nanostructures including spheres, cylinders, and lamellae, of which sizes are typically in the range of a few tens of nanometers.[16,17] Thus, nanostructures of block copolymers can be applied to efficient generation of functional nanopatterns without heavy lithographic tools.[18,19]

In this work, we first demonstrated the creation of fluorescent nanopatterns because top-down lithography or bottom-up assembly alone cannot efficiently produce fluorescent

patterns in the nanometer range. For effective production of fluorescent nanopatterns without a lithographic tool, we synthesized diblock copolymers having fluorophores in one of the blocks by the reversible addition fragmentation chain transfer (RAFT) polymerization. Since fluorophores are covalently linked to one of the blocks, they assembled only in the nanodomains of that block by solvent vapor annealing, resulting in hexagonal or linear fluorescent nanopatterns. However, these fluorescent nanodomains are embedded in the matrix of the other block of copolymers. Thus, by etching the matrix block selectively, we finally obtained pure fluorescent nanopatterns with topographic features. In addition, we were able to modify fluorescence of the nanopattern by placing Au nanorods in the nanometer-sized valley of the pattern. This result implies a potential application in detection of nanometer-sized objects with fluorescent topographic nanopatterns.

2. Experimental

Materials

All chemicals were commercially available and were used as received unless noted. 2,2'-Azoisobutyronitrile (AIBN) was recrystallized from ethanol. Methylmethacrylate (MMA), styrene, and 4-vinylbenzyl chloride were distilled under reduced pressure. All solvents were purified by common procedures.

Synthesis of Diblock Copolymers with Benzyl Chloride Units

For polymerization, a Schlenk tube equipped with a stir bar was loaded with 10.0 g (99.9 mmol) of MMA, 6.8 mg (0.025 mmol) of cumyldithiobenzoate, and 0.41 mg (0.0025 mmol) of AIBN. Then, air was exchanged with argon by three freeze–thaw cycles. Polymerization of MMA was carried out at 70 ^{o}C for 48 h with vigorous stirring. Polymers

were purified by precipitating them into methanol. Two more precipitations were performed from their THF solutions. After drying at 30 ^{o}C overnight in vacuum, 3.5 g (70%) of poly(methylmethacrylate) (PMMA) was obtained in pink powder. The number average molecular weight is 127,000 g/mol with PS standards and 141,000 g/mol with PMMA standards. The polydispersity index is 1.08 (GPC with PS standards, Supporting Information, Figure S1). To synthesize poly(methylmethacrylate)-b-poly(styrene-r-(4-vinylbenzylchloride)) (PMMA-b-P(S-r-4VBC)) diblock copolymers, the PMMA macro chain transfer agent (1.0 g, 0.0079 mmol), AIBN (0.3 mg, 0.00079 mmol), styrene (8.72 g, 8.4 mmol), and 4-vinylbenzyl chloride (1.28 g, 0.84 mmol) were added together in a Schlenk tube. Oxygen was exchanged by argon in three freeze–thaw cycles and polymerization was carried out at 70 ^{o}C for 22 h. Copolymers were purified by precipitation in methanol three times. To remove unlinked P(S-r-4VBC) polymers, Soxhlet with cyclohexane was performed and then 1.7 g of PMMA-b-P(S-r-4VBC) in pale pink powder was obtained. The number average molecular weight is 263,000 g/mol and the polydispersity index is 1.13 (GPC, Supporting Information, Figure S1 and NMR, Supporting Information, Figure S2).

Synthesis of Fluorophore-Functionalized Diblock Copolymers

To attach a fluorophore to the diblock copolymer, post-polymerization modification was carried out. PMMA-b-P(S-r-4VBC) (180 mg), rhodamine 110 hydrochloride (46 mg, 0.125 mmol), and triethylamine (116 mg, 0.43 mmol) were dissolved in DMF (15 ml) and stirred under argon at 50 ^{o}C for 2 days. Then, the solution was extracted by distilled water and chloroform. Unreacted rhodamine 110 was dissolved in distilled water and fluorophore-functionalized copolymers were dissolved in chloroform. After evaporating chloroform, the solution was precipitated in methanol and copolymers were filtered and washed with

methanol many times. The copolymer product in reddish pink powder was finally obtained (NMR, Supporting Information, Figure S4).

Fabrication of Fluorescent Topographic Nanopatterns

Silicon wafers and quartz plates were cleaned in a piranha solution (70/30 v/v of concentrated H_2SO_4 and 30% H_2O_2) at 90 ^oC for 30 min, thoroughly rinsed with deionized water several times, and then blown dry with nitrogen. After cleaning, substrates were immediately used. A thin film on a substrate was fabricated by spin coating (typically at 2000 rpm for 60 s) from a toluene solution (1.0~1.5 wt%) of a mixture of PMMA-b-P(S-r-4VBC-r-Rho) and PMMA-b-PS (5,000 g/mol for each block) with a weight ratio of 10:4. A thin film was exposed to saturated vapor of acetone or chloroform in a closed glass jar at room temperature for 1 h (acetone) or 13 h (chloroform). After annealing, the sample was removed to ambient atmosphere and dried. PMMA domains in annealed films were etched by oxygen plasma (80 W, 38 mTorr) for 10 s (an acetone-annealed film) and 13 s (a chloroform-annealed film).

Synthesis of Au Nanorods

Au nanorods were synthesized by the seeded-growth method with binary surfactants of hexadecyltrimethylammonium bromide and sodium oleate as described in the literature,[27] which have the diameter of ~33 nm and the length of ~96 nm (Supporting Information, Figure S5). They were spin-coated at 1500 rpm for 60 s on a thin film of the copolymer with or without a topographic nanopattern. The film without a topographic feature was treated with oxygen plasma (80 W, 38 mTorr) for 2 s before spin coating of Au nanorods to make the surface hydrophilic.

Characterization

NMR spectra were obtained on a Varian NMR System (500 MHz). Gel permeation chromatography (GPC) was carried out on a Waters system (1515 pump, 2414 refractive index detector) with a Shodex GPC LF-804 column. Atomic force microscopy (AFM Nanoscope IIIA, Digital Instrument) was used in tapping mode with Si cantilevers. Transmission electron microscopy (TEM) analysis was performed on a Hitachi 7600 operating at 100 kV. UV-Vis absorption spectra were recorded on a Varian Cary-5000 spectrophotometer. Steady-state fluorescence was measured on an Acton Spectra Pro 2300i with a He-Cd laser (442 nm) as the excitation source.

3. Results and Discussion

To demonstrate fluorescent nanopatterns, we first synthesized PMMA-b-P(S-r-4VBC) diblock copolymers by the RAFT polymerization as shown Figure 1. 4-vinlybenzyl chloride (4VBC) units were randomly included in the polystyrene (PS) block and then reacted with Rhodamine 110, a fluorescent dye, which contains the primary amine functionality. We included ~10 mol% of 4VBC in the PS block to have sufficient fluorescence but not to affect overall behaviors of the PS block. For the other block, poly(methyl methacrylate) (PMMA) was selected because it can be selectively etched. PMMA was synthesized first and used as a macro chain transfer agent to attach the second block of P(S-r-4VBC). The number average molecular weight and polydispersity index of PMMA-b-P(S-r-4VBC) are 264,000 g/mol and 1.13, respectively (Supporting Information, Figure S1). The mole ratio between two blocks is 1:1 (Supporting Information, Figure S2). The NMR result also confirmed 10.4 mol% of 4VBC in the PS block (Supporting Information, Figure S2). Since benzyl chloride can react with primary amine,[20,21] rhodamine 110, which shows absorption at 496 nm and emission at

520 nm (Supporting Information, Figure S3), was selected as a representative fluorophore and covalently linked to the P(S-r-4VBC) block as shown in Figure 2. We confirmed that 7.8 mol% of rhodamine 110 was attached to the P(S-r-4VBC) block (Supporting Information, Figure S4). This fluoropore-functionalized diblock copolymers synthesized by RAFT enable the fabrication of a fluorescent nanopattern without a lithographic tool because fluorophores covalently linked to one of the blocks can spontaneously assemble only in the nanodomain of that block by solvent vapor annealing.

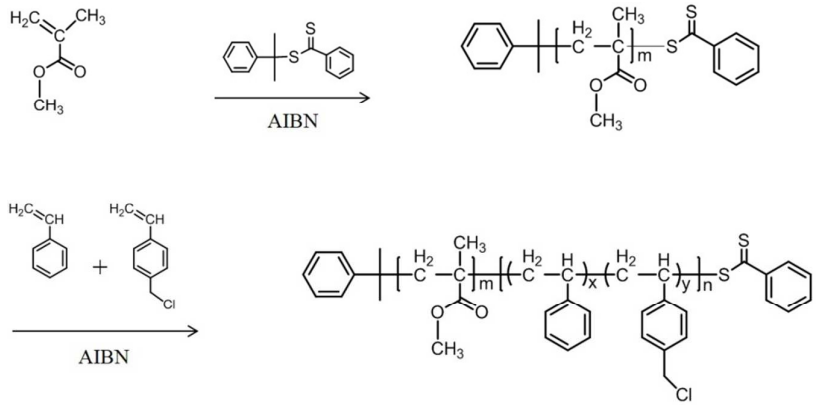

Figure 1. Synthesis of PMMA-b-P(S-r-4VBC).

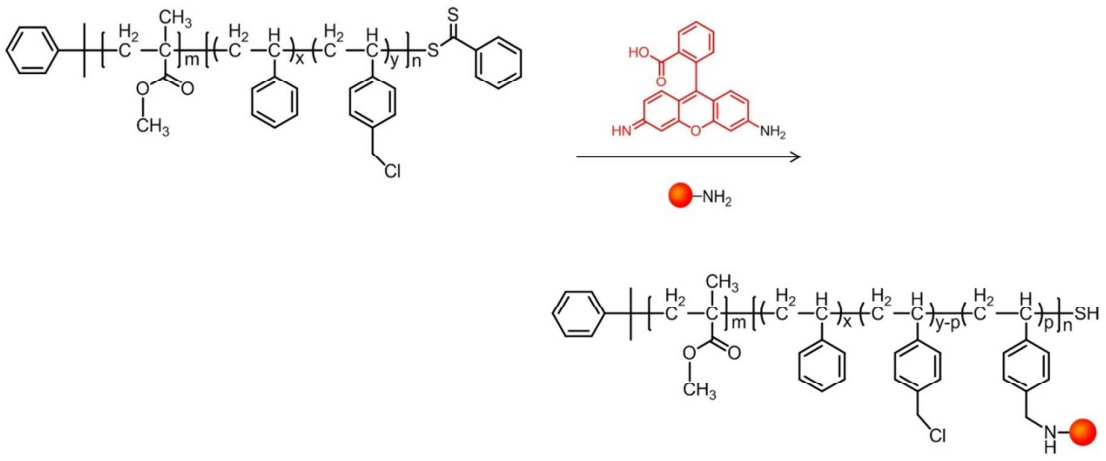

Figure 2. Synthesis of rhodamine-functionalized PMMA-b- P(S-r-4VBC-r-Rho).

To produce fluorescent nanopatterns, we first annealed a thin film of PMMA-b-P(S-r-4VBC-r-Rho) by acetone vapor, instead of thermal annealing, to avoid undesirable changes of fluorophores at high temperatures. Since we employed a relatively large molecular weight (264,000 g/mol) of the fluorophore-functionalized copolymer, PMMA-b-PS with a low molecular weight (10,000 g/mol) was mixed with the copolymer to promote evolution of nanostructures during the solvent annealing as demonstrated in the literature.[22]

In Figure 3, we can find a hexagonally ordered nanopattern in an acetone-annealed PMMA-b-P(S-r-4VBC-r-Rho) thin film. In the TEM image (Figure 3a), dark gray dots and white regions between them correspond to P(S-r-4VBC-r-Rho) and PMMA, respectively, because PMMA generally appears bright in TEM images due to thinning by the electron beam.[23] In the AFM image (Figure 3b), bright nanopatterns are also discernible, which are perpendicular cylinders of the P(S-r-4VBC-r-Rho) block in a hexagonal array, embedded in the matrix of the PMMA block. The diameter and center-to-center distance (domain spacing) of these cylindrical nanostructures are ~62 nm and ~83 nm, respectively.

Acetone can selectively swell the PMMA block of PMMA-b-P(S-r-4VBC-r-Rho) copolymers so that the formation of cylindrical nanostructures of the P(S-r-4VBC-r-Rho) block in the PMMA matrix is reasonable even though the mole ratio between two blocks is 1:1. Perpendicular cylinders are typically obtained in a thin film of diblock copolymers when the film thickness is smaller than a half of the domain spacing.[24] Thus, the perpendicular cylinders in Figure 3 can be understood because the film has a smaller thickness (~32 nm) than a half of the domain spacing (~41.5 nm). Therefore, we produced a nanopattern of hexagonally ordered cylinders, which are functionalized with red-emitting fluorophores, by acetone vapor annealing on a thin film PMMA-b-P(S-r-4VBC-r-Rho) copolymers as shown in the schematic illustration in Figure 3b.

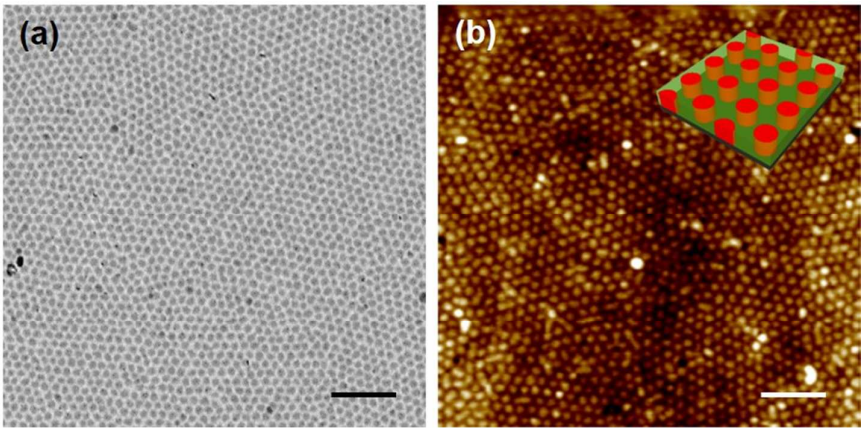

Figure 3. PMMA-b-P(S-r-4VBC-r-Rho) thin film after acetone vapor annealing: (a) TEM image; (b) AFM image. The scale bars are 500 nm.

To generate a topographic nanopattern, we removed the PMMA matrix, in which the fluorophore-functionalized cylinders are hexagonally arranged, in a thin film of PMMA-b-P(S-r-4VBC-r-Rho) copolymers. Oxygen plasma etching was performed directly on the thin film, which etched the PMMA block faster than the other block, resulting in a topographic nanopattern of cylinders functionalized with red-emitting fluorophores (Figure 4). The height of cylinders becomes ~8 nm, indicating that most of PMMA domains were removed when the film thickness before etching (~32 nm) is considered. We confirmed red-color emissions from the topographic nanopattern as shown in the PL spectrum of Figure 4b. Thus, we generated a fluorescent topographic nanopattern from a thin film of PMMA-b-P(S-r-4VBC-r-Rho) copolymers which is illustrated in Figure 4a. We note that UV irradiation followed by washing with acetic acid can selectively remove PMMA domains in a diblock copolymer containing a PMMA block without scarifying the film thickness.[25] However, this process, particularly UV irradiation, can damage fluorescent characteristics of fluorophore-functionalized copolymers.

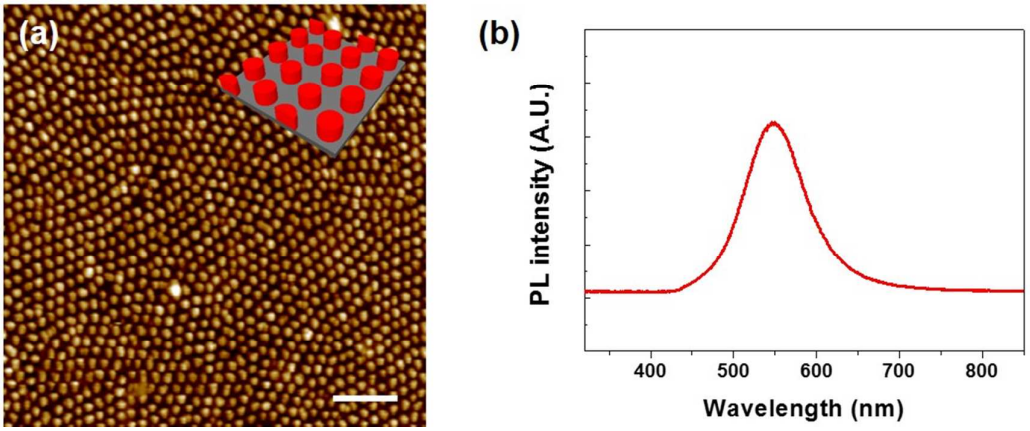

Figure 4. Fluorescent topographic nanopattern from acetone-annealed PMMA-b-P(S-r-4VBC-r-Rho) after etching the PMMA matrix: (a) AFM image; (b) PL spectrum. The scale bar is 500 nm.

By annealing a thin film of PMMA-b-P(S-r-4VBC-r-Rho) copolymers with chloroform instead of acetone, we obtained a fluorescent nanopattern consisting of fluorophore-functionalized cylinders parallel to the film plane as shown in Figure 5. In both TEM and AFM images, we can find parallel cylinders with the diameter of ~61 nm and the center-to-center distance of ~84 nm, which are almost identical to those of perpendicular cylinders in Figure 3. In general, cylindrical nanostructures are oriented parallel to the substrate in thin films of diblock copolymers by solvent vapor annealing with the film thickness greater than a half of the domain spacing.[24] The film thickness (~48 nm) in Figure 5 is larger than a half of the domain spacing (~42.5 nm). In addition, chloroform can dissolve both blocks of PMMA-b-P(S-r-4VBC-r-Rho) but prefer the PMMA block to the other block.[24] These conditions can explain cylindrical nanostructures parallel to the film plane in a thin film of PMMA-b-P(S-r-4VBC-r-Rho) annealed by chloroform. Thus, we generated a nanopattern of fluorophore-functionalized cylinders oriented parallel to the substrate as

shown in the schematic illustration in Figure 5b.

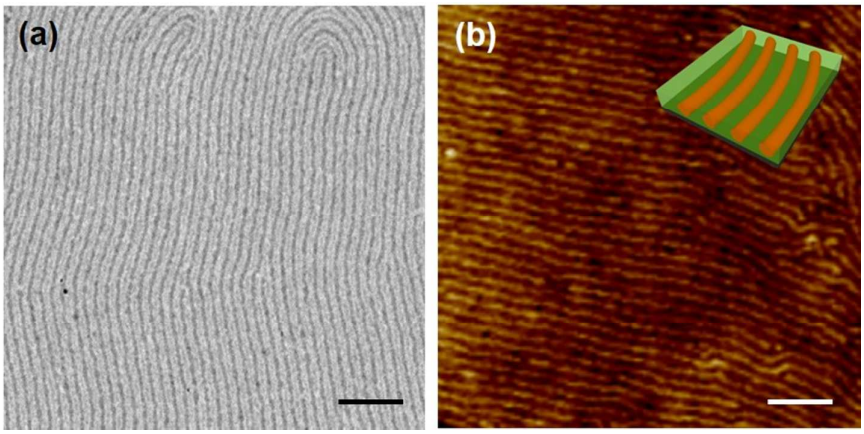

Figure 5. PMMA-b-P(S-r-4VBC-r-Rho) thin film after chloroform vapor annealing: (a) TEM image; (b) AFM image. The scale bars are 500 nm.

As the previous case of cylindrical nanostructures in hexagonal order, we produced a topographic nanopattern by removing the PMMA matrix in a thin film of PMMA-b-P(S-r-4VBC-r-Rho) copolymers after chloroform vapor annealing. By oxygen plasma etching, we obtained a topographic nanopattern of parallel cylinders functionalized with red-emitting fluorophores as shown in the AFM image of Figure 6, in which the thickness of each cylinder is ~16 nm. We also confirmed red-color emissions from this topographic nanopattern as shown in the PL spectrum of Figure 6b. Therefore, by chloroform annealing, a fluorescent topographic nanopattern of parallel cylinders was created (schematic illustration in Figure 6a), whereas that of hexagonally ordered cylinders was obtained by acetone annealing (schematic illustration in Figure 4a), using the same fluorophore-functionalized copolymer.

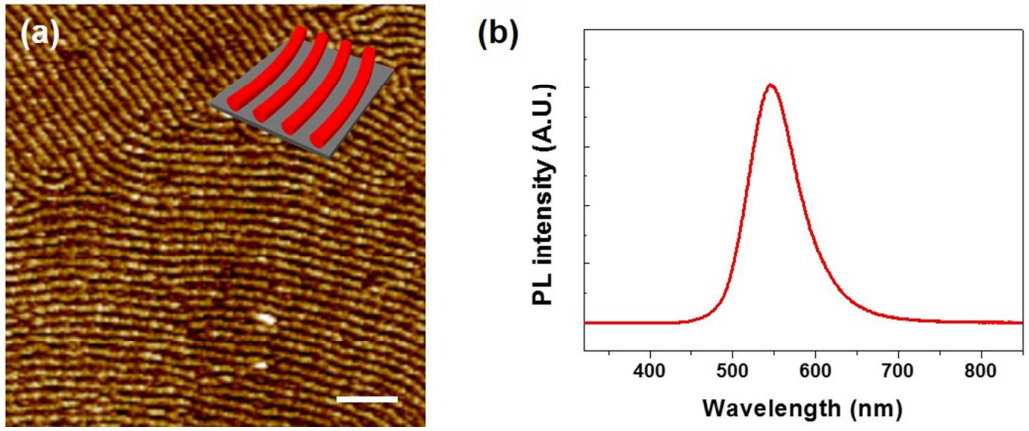

Figure 6. Fluorescent topographic nanopattern from chloroform-annealed PMMA-b-P(S-*r*-4VBC-*r*-Rho) after etching the PMMA matrix: (a) AFM image; (b) PL spectrum. The scale bar is 500 nm.

To examine a value of a fluorescent topographic nanopattern, we introduced Au nanorods on the fluorescent nanopattern of parallel cylinders with and without a topographic feature. We employed Au nanorods having the diameter of ~33 nm and the length of ~96 nm (Supporting Information, Figure S5), which can be fit into the valley of the topographic nanopattern because the diameter is smaller than the width of the valley (~44 nm). In the AFM images of Figure 7, most of Au nanorods are aggregated on a thin film of PMMA-b-P(S-r-4VBC-r-Rho) without a topographic feature, whereas Au nanorods exist individually and many of them follow the cylindrical line on the topographic nanopattern. From the height profile of single nanorod on the film without a topographic pattern (Figure 7a), the thickness of a nanorod (~31 nm) is almost the same as its diameter (~33 nm), indicating that the nanorod resides on the top of the film. In contrast, the thickness of the nanorod on the topographic pattern (~17 nm) is close to a half of its diameter, which confirms that the nanorod fits into the valley of the topographic pattern. These Au nanorods in the valleys of

the topographic pattern increased emissions of the fluorescent nanopattern (Figure 8b) due to the near-field scattering effect of Au nanorods[26] which exist very next to the fluorophore-functionalized cylinders. However, no enhancement of the emission was observed in the case of Au nanorods on the top of the fluorescent nanopattern without a topographic feature (Figure 8a). When a spacer layer of poly(acrylic acid) (8,000 g/mol) with the thickness of 7.2 nm was inserted between Au nanorods and the fluorescent nanopattern, no enhancement of the emission was observed (Supporting Information, Figure S6), implying that the distance between Au nanorods and the fluorescent nanopattern is crucial for near-field effects of Au nanorods. Thus, a fluorescent topographic nanopattern can find a potential application of detection or sensing with nanometer-sized objects. We note that the nanopatterns with or without Au nanorods did not show enough absorption in UV-Vis spectroscopic measurements because they were too thin.

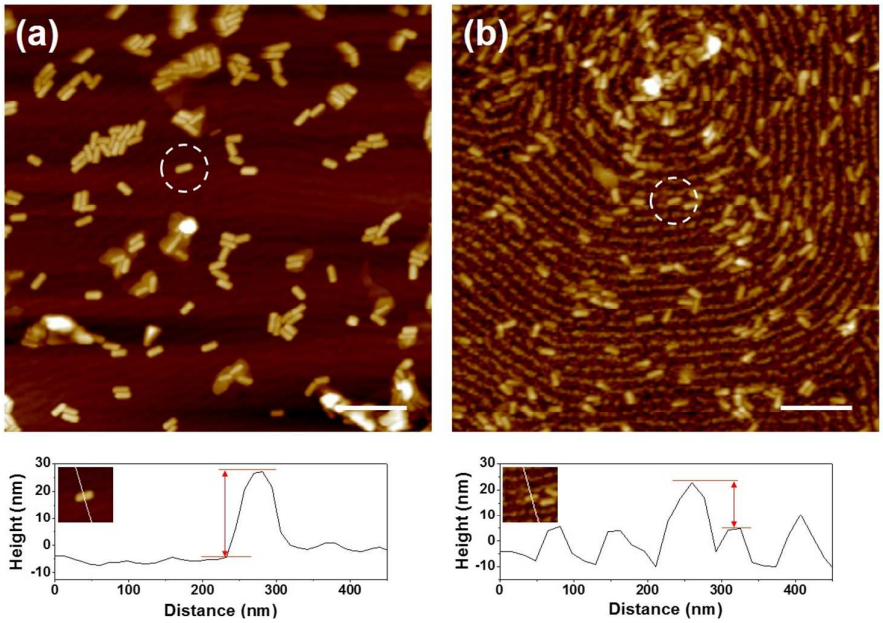

Figure 7. AFM images of Au nanorods on PMMA-b-P(S-r-4VBC-r-Rho) thin films: (a)

without topographic pattern; (b) with topographic pattern. A height profile of single Au nanorod marked by the white circle is given under each image. The scale bars are 500 nm.

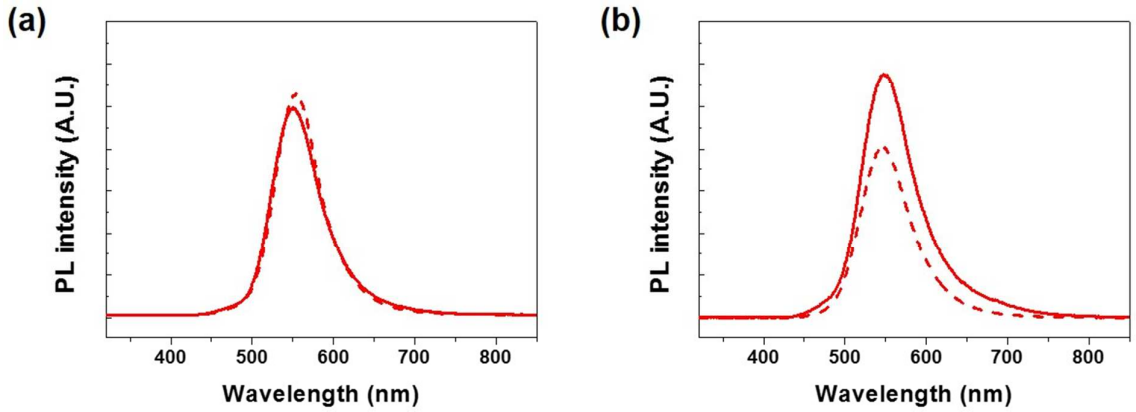

Figure 8. PL spectra of PMMA-b-P(S-*r*-4VBC-*r*-Rho) thin films with Au nanorods (solid line) and without Au nanorods (dashed line): (a) without topographic pattern; (b) with topographic pattern.

4. Conclusions

We synthesized PMMA-b-P(S-*r*-4VBC-*r*-Rho), a fluorophore-functionalized diblock copolymer, by the RAFT polymerization. Acetone vapor annealing on a thin film of the copolymer generated a nanopattern of fluorescent cylinders in hexagonal order. In contrast, a fluorescent nanoppattern of parallel cylinders was produced by chloroform vapor annealing. Then, by etching the PMMA block of the copolymer, we were able to create topographic nanopatterns of red-emitting cylinders in hexagonal order or in parallel lines. Furthermore, emission of the topographic nanopattern was enhanced by placing Au nanorods selectively in the nanometer-sized valley of the pattern, implying that a fluorescent topographic nanopattern can be utilized in detection or sensing with nanometer-sized objects

Acknowledgements

This work was supported by Mid-career Researcher Program through NRF grant funded by the MSIP (No. 2014-002290).

References

1. R. C. Somers, M. G. Bawendi and D. G. Nocera, *Chem. Soc. Rev.,* 2007, **36**, 579 – 591.

2. S. A. Corr, Y. P. Rakovich, Y. K. Gun'ko, *Nanoscale Res. Lett*, 2008, **3**, 87 - 104.

3. P. Sharma, S. Brown , G. Walter, S. Santra, B. Moudgil, Advances in Colloid and Interface Science 2006, 123-126, 471 - 485.

4. D. R. Larson, W. R. Zipfel, R. M. Williams, S. W. Clark, M. P. Bruchez, F. W. Wise, W. W. Webb, *Nature*, 2003, **300**, 1434 - 1436.

5. U. Resch-Genger, M. Grabolle, S. Cavaliere-Jaricot, R. Nitschke and T. Nann, *Nature methods*, 2008, **5**, 763 - 775.

6. I. L. Medintz, H. T. Uyeda, E. R. Goldman and H. Mattoussi, *Nature materials*, 2005, **4**, 435 - 446.

7. A. Burns, H. Owb and U. Wiesner, *Chem. Soc. Rev.*, 2006, **35**, 1028 - 1042.

8. M. Wu, H. Shi, J. Xu and H. Chen, *Chem. Commun.*, 2011, **47**, 7752 - 7754.

9. E. Han, L. Ding, H. Lian and H. Ju, *Chem. Commun.*, 2010, **46**, 5446 - 5448.

10. M. J. Hampton, J. L. Templeton, and J. M. DeSimone, *Langmuir*, 2010, **26**, 3012 - 3015.

11. L. A. Kim, P. O. Anikeeva, S. A. Coe-Sullivan, J. S. Steckel, M. G. Bawendi, and V. Bulovic, *Nano Lett.*, 2008, **8**, 4513 - 4517.

12. S. Jaffar K. T. Nam, A. Khademhosseini, J. Xing, R. S. Langer, and A. M. Belcher, *Nano lett.*, 2004, **4**, 1421 - 1425.

13. J. Kim, T. Chang, J. Kang, K. H. Park, D. Han, and K. Ahn, *Angew. Chem. Int. Ed.*, 2000,

39, 1780 - 1782.

14. G. Pistolis, S. Boyatzis, M. Chatzichristidi, and P. Argitis, *Chem. Mater.*, 2002, **14**, 790 - 796.
15. Seo, H. Shin, C. Park, H. Lim, and E. Kim, *Macromol. Res.*, 2013, **21**, 3523.
16. S. B. Darling, *Prog. Polym. Sci.*, 2007, **32**, 1152 - 1204.
17. S. Förster and M. Antonietti, *Adv. Mater.*, 1998, **3**, 195 - 217.
18. C. J. Hawker, T. P. Russell, *MRS bulletin*, 2005, **30**, 952 - 966.
19. H. Kim, S. Park, and W. D. Hinsberg, *Chem. Rev.*, 2010, **110**, 146 - 177.
20. W. H. Yu, E. T. Kang, and K. G. Neoh, *Ind. Eng. Chem. Res.*, 2004, **43**, 5194 - 5202.
21. D. S tefanec, P. Krajnc, *Reactive & Functional Polymers*, 2005, **65**, 37 - 45.
22. D. O. Shin, J. Jeong, T. H. Han, C. M. Koo, H. Park, Y. T. Lim and S. O. Kim, *J. Mater. Chem.*, 2010, **20**, 7241 - 7247.
23. B. L. Carvalho, E. L. Thomas, *Phys. Rev. Lett.*, 1994, **73**, 3321 - 3324.
24. Y. Xuan, J. Peng, L. Cui, H. F. Wang, B. Li, and Y. Han, *Macromolecules*, 2004, **37**, 7031 - 7307.
25. T. Thurn-Albrecht, R. Steiner, J. DeRouchey, C. M. Stafford, E. Huang, M. Bal, M. Tuominen, C. J. Hawker, and T. P. Russell, *Adv. Mater.*, 2000, **12**, 787 - 791.
26. K. Lee and M. A. El-Sayed, *J. Phys. Chem. B*, 2005, **109**, 20331 - 20338.
27. X. Ye, C. Zheng, J. Chen, Y. Gao, and C. B. Murray, *Nano Lett.,* 2013, **13**, 765 - 771.